Microchim Acta (2015) 182:281–288
DOI 10.1007/s00604-014-1329-z

ORIGINAL PAPER

Dipeptidyl peptidase-IV activity assay and inhibitor screening using a gold nanoparticle-modified gold electrode with an immobilized enzyme substrate

Juan Zhang · Ying Liu · Jun Lv · Ya Cao · Genxi Li

Received: 10 April 2014 / Accepted: 15 July 2014 / Published online: 22 July 2014

Abstract We report on an electrochemical biosensor for the determination of the activity of dipeptidyl peptidase-IV (DPP-IV), and on a method for screening the effect of its inhibitors. An enzyme substrate (Fc-peptide) was immobilized on the surface of a gold electrode, and double signal amplification was accomplished via an additional layer consisting of phenyl rings and gold nanoparticles. The activity of DPP-IV was determined at levels as low as 39 $nU \cdot mL^{-1}$ and over a linear detection range as wide as from 0.5 $\mu U \cdot mL^{-1}$ to 2.5 $mU \cdot mL^{-1}$. The inhibitory effects of diprotin A and the His-Leu dipeptide on the activity of DPP-IV also were tested and gave IC_{50} values of 93.5 and 95.5 μM, respectively. The assay is rapid, precise and selective. It may be extended to other peptidases and, possibly, proteases and their inhibitors.

Keywords DPP-IV · Inhibitor · Fc-pepetide · Electrochemical biosensor

Introduction

Type II diabetes mellitus (T2DM) is a serious metabolic disorder, which is diagnosed on the basis of sustained hyperglycemia [1]. Intensive control on blood glucose level is always an effective way to halt T2DM development [2]. In the treatment of T2DM, protein dipeptidyl-peptidase IV (DPP-IV) inhibitor is a new leading class of oral anti-diabetic agents. The inhibitor can be able to avoid safety and tolerability issues of conventional agents. Animal experiments and human trials have demonstrated that specific DPP-IV inhibition may increase the half-life of total circulating glucagon-like peptidase-1, decreases plasma glucose, and improves impaired glucose tolerance [3]. So, it has been highly required to develop the method for the analysis of DPP-IV activity and its inhibitor screening.

DPP-IV, a membrane-bound serine proteinase, was discovered by Hopsu Havu and Glenner in rat liver homogenates [4]. The enzyme cleaves peptides with Pro or Ala residues in the second amino terminal position [5]. Currently, spectrophotometry and HPLC methods have been applied to analyze DPP-IV activity and screen the inhibitors. So, Aertgeerts et al. have determined the effect of N-linked glycosylation of DPP-IV on enzyme activity by fluorospectrometry [6, 7]. Hama et al. have purified DPP-IV from human kidney by affinity chromatography [7]. Kim et al. have studied saxagliptin, an inhibitor of DPP-IV, by spectrometry [8]. These methods have the disadvantage that they require the coloration of the test solution, fluorescent labels, and sophisticated instrumentations, which are high-cost and time-consuming.

Electrochemical technique does not have above problems, and it has been demonstrated to be simple and cost-effective [9, 10]. However, electrochemical method has not been established to determine DPP-IV activity and screen its inhibitor. Moreover, in the previous studies, the synthetic exogenous compounds used as the substrate of DPP-IV for spectrometric measurement may lead to inaccuracy in the analysis for the enzyme activity and inhibition effect. So, it is necessary to choose endogenous compound as DPP-IV substrate, in order to enhance the accuracy.

Electronic supplementary material The online version of this article (doi:10.1007/s00604-014-1329-z) contains supplementary material, which is available to authorized users.

J. Zhang · Y. Liu · J. Lv · Y. Cao · G. Li
Laboratory of Biosensing Technology, School of Life Sciences, Shanghai University, Shanghai 200444, People's Republic of China

G. Li (✉)
State Key Laboratory of Pharmaceutical Biotechnology, Department of Biochemistry, Nanjing University, Nanjing 210093, People's Republic of China
e-mail: genxili@nju.edu.cn

Ferrocence (Fc) molecule attached to the distal end of molecular wires have been commonly used for fundamental electrochemistry and potential applications [11]. Meanwhile, Fc-peptide has displayed a moderate stability, and a significant fraction of Fc-peptide chains immobilized on an electrode surface appears to be cleavable by protease [12]. So, the endogenous opioid peptide of DPP-IV, endomorphine-2 (Tyr-Pro-Phe-Phe-NH_2) [13], might be conjugated with Fc molecule, and the Fc-peptide bound to gold electrode may allow for identifying DPP-IV activity and screening of its inhibitors.

It has been proved that good conductivity can be achieved through direct bonding of the phenyl ring to gold surface [14]. The phenyl ring can be grafted onto gold electrode through electrochemical reduction of in situ generated aminophenyl diazonium cations [15]. Meanwhile, it has been known that the fabrication of nanostructured electrodes may allow for immobilizing a higher amount of biocatalyst per geometric electrode area unit, thus leading to higher catalytic current densities [16, 17]. Therefore, it would be a good way to acquire high sensitivity through direct grafting of phenyl ring onto the surface of gold electrode, followed by modification of gold nanoparticles (AuNPs), to achieve double signal amplification.

Based on the above rationale, we have developed an electrochemical biosensor for detection of DPP-IV activity and screening of its inhibitors. In this sensor, the endogenous peptide is linked with Ferrocenecarboxylic acid to form a Fc-peptide, which is used for the substrate of DPP-IV. Meanwhile, since the surface of gold electrode has been covered by a layer of phenyl ring through electrochemical reduction of in situ generated aminophenyl monodiazonium cations, followed by the linkage of AuNPs, the enzymatic activity can be not only determined by the current change of the electrochemical response due to the hydrolysis of the substrate Fc-peptide in the presence of DPP-IV, but the signal readout can also be highly amplified. Furthermore, cyclic voltammetry (CV) and square wave voltammetry (SWV) have been used to screen its inhibitors in this work.

Experimental

Chemicals and materials

The substrate ferrocene-peptide (Fc-Tyr-Pro-Phe-Phe) and the inhibited peptides (diprotin A and His-Leu) were synthesized and purified (>98 % purity) by China Peptides Co., Ltd. (Shanghai, China, http://www.chinapeptides.com/indexe.php). Dipeptidyl peptidase-IV (EC 3.4.14.5), 3-(4-aminophenyl)propionic acid (APPA), $HAuCl_4{\cdot}4H_2O$, cysteamine, 1-ethyl-3-(3-dimethylaminopropyl) carbodiimide hydrochlo-ride (EDC), N-hydroxysuccinimide (NHS), and 4,7,10-trioxa-1,13-tridecanediamine were purchased from Sigma-Aldrich (Shanghai, China, http://www.sigmaaldrich.com/china-mainland.html).

The buffer solutions employed are as follows. Peptide storage buffer: 20 mM HEPES (pH 7.0). Enzymatic buffer for DPP-IV: 100 mM Tris–HCl. Electrode washing buffer: 20 mM Tris–HCl, 5 mM $MgCl_2$, 0.1 M NaCl and 1 % Tween-20 (pH 7.4). Solution for electrochemical impedance spectroscopy (EIS): 5 mM $[Fe(CN)_6]^{3-/4-}$ with 1 M KNO_3. Solution for cyclic voltammetry (CV) and Square-wave voltammetry (SWV): 1 M $NaClO_4$. All buffers and aqueous solutions were prepared with ultrapure water, which was purified with a Millipore Milli-Q water purification system (Branstead, USA) to a specific resistance of 18 MΩ cm.

Synthesis of cysteamine functionalized AuNPs

The cysteamine functionalized AuNPs (CA-AuNPs) were synthesized by sodium borohydride reduction of hydrogen tetrachloroaurate (III) trihydrate in the presence of cysteamine according to documented protocols [18]. Briefly, 400 μL of 213 mM cysteamine was added to 40 mL of 1.42 mM $HAuCl_4{\cdot}4H_2O$. After stirring for 20 min at room temperature, 10 μL of 10 mM $NaBH_4$ solution was added to the mixture with vigorous stirring for 10 min in the dark. Sodium borohydride was dissolved in cold deionized water immediately before use. The color of mixture changed from yellow to brown. After further slow stirring, the CA-AuNPs solution was collected by centrifugation at 8,000 rpm for 10 min. The red precipitate was washed, centrifuged, and dispersed in ultrapure water. After that, the CA-AuNPs solution was stored in the dark at 4 °C.

Electrode surface treatment and modification

The gold electrode was polished sequentially with 1.0 and 0.3 μm alumina slurry, followed by ultrasonic cleaning in ethanol and ultrapure water. Subsequently, the gold electrode was cleaned in piranha solution (98 % H_2SO_4 : 30 % H_2O_2=3 : 1) for 2 min. Afterward, the gold electrode was washed thoroughly with amounts of ultrapure water and dried under nitrogen gas. At last, the surface was electrochemically cleaned in 0.5 M H_2SO_4 to remove any remaining impurities.

Gold electrodes were firstly modified with APPA by in situ diazonium reduction experiments [19]. APPA was diazotated in an aqueous solution of 5 mM HCl and 5 mM $NaNO_2$, which was deaerated by bubbling with ultrapure nitrogen gas for 5 min prior to each experiment. Then the electrode was dipped in diazonium solution, and cyclic voltammetric experiment was conducted from 0 to −600 mV at a scan rate of 100 $mV{\cdot}s^{-1}$. After the formation of phenyl ring layer, the electrode was fully rinsed with ultrapure water to remove unbound molecules. Subsequently, the electrode was dipped

in solutions of 0.4 M EDC and 0.1 M NHS for 30 min to activate carboxyl group and successively immersed in CA-AuNPs solution for 2 h. Afterward, the electrode was incubated with succinic anhydride (3 %) for 3 h, the solutions of 0.4 M EDC and 0.1 M NHS for 30 min, and 4,7,10-trioxa-1,13-tridecanediamine (3 %) for 2 h. After washing with ultrapure water, the electrode was immersed into 80 μL Fc-peptide solution, including 10 μL 0.4 M EDC and 10 μL 0.1 M NHS, overnight. Finally, the electrode was treated with 1 mM 6-mercapto-1-hexanol for 1 h, and immersed in 1 % Tween 20 solution to avoid the nonspecific absorption.

Proteolytic reaction of Fc-peptide on the surface of electrode

The surface reaction of immobilized Fc-peptide catalyzed by DPP-IV was conducted as follows. 100 μL DPP-IV solution was pre-activated at 37 °C for 5 min. The Fc-peptide modified electrode was immersed in the solution at different temperature for a given time period. Then the electrode was thoroughly rinsed with the washing buffer to terminate the reaction.

Inhibition of DPP-IV activity

For the measurement of enzymatic inhibitor screening, diproin A and His-Leu were chosen as representative compound. The mixed solution of 50 μL DPP-IV (pH 7.8) and 50 μL inhibitor was incubated at 37 °C for 1 h. The modified electrode was immersed into the reaction mixture at 37 °C for 1 h. The inhibitory ratio (%) of diproin A or His-Leu on enzymatic activity was expressed as follows:

$$\text{Inhibitory ratio}(\%) = (I_3 - I_2) \Big/ (I_1 - I_2) \times 100\ \%$$

where I_1 was the peak current obtained in absence of enzyme, I_2 was the peak current obtained in presence of enzyme, I_3 was the peak current obtained with both enzyme and inhibitor.

Electrochemical measurements

Square-wave voltammetric and cyclic voltammetric measurements were performed with an electrochemical analyzer CHI 1040B (CH Instruments, Shanghai, China) and electrochemical impedance spectroscopy (EIS) measurements were performed using CHI660C (CH Instruments, Shanghai, China). A three-electrode configuration was employed, consisting of the modified Fc-peptide electrode (2 mm diameter) serving as a working electrode, while saturated calomel electrode (SCE) and platinum wire served as the reference and counter electrode, respectively. Cyclic voltammograms were obtained over the potential scan range from 0 to 0.8 V at the scan rate of 100 mV/s. Square-wave voltammograms were recorded in the potential scan range from 0.3 to 0.7 V. EIS was performed by applying a bias potential of 0.224 V vs. SCE and 5 mV amplitude in the frequency range from 0.1 Hz to 10 kHz.

Results and discussions

Fabrication of the Fc-peptide modified gold electrode has been shown in Scheme 1a. Firstly, phenyl ring is directly grafted onto the gold electrode surface by electrochemical reduction of in situ generated aminophenyl monodiazonium cations. As shown in Fig. S1 (Electronic Supplementary Material, ESM), a pair of well-defined redox peaks can be observed in the first circle (a), which is assigned to the formation of the aryl radical that is subsequently attached to the electrode surface. In the consecutive cycles (b and c), the cathodic peak slightly shifts to more negative direction and the peak current changes to be lower, due to the passivation of the gold electrode as a result of the formation of a grafted ring [20]. Afterwards, CA-AuNPs are immobilized on the electrode surface by covalent bonding between the carboxylic acid group of the modified electrode surface and the amine group of the nanoparticle surface. AuNPs have an evident effect of signal amplification. As shown in Fig. S2 (ESM), it can be observed that the peak current on Fc-peptide/CA/Au electrode is lower than that on Fc-peptide/CA-AuNPs/APPA/Au electrode. After that, the chain is lengthened through the formation of two amide bonds, which consecutively forms through chemical reaction of the amine group of the nanoparticle surface and succinic anhydride, and the reaction of the carboxyl group of the modified electrode and the amine group of 4,7,10-trioxa-1,13-tridecanediamine. Finally, Fc-peptide, the substrate of the enzyme, is covalently attached to the modified gold electrode surface via the amide bond.

The mechanism of the method for the detection of DPP-IV activity and screening of its inhibitor has been shown in Scheme 1b. Because DPP-IV may cleave the peptides with Pro or Ala residues in the second amino terminal position, the Pro residue of Fc-peptide can be cleaved in the presence of enzyme. As a result, the Fc moiety is released from the electrode surface into the bulk solution, leading to the decrease of the redox signal of Fc. On the contrary, in the presence of both the enzyme and the inhibitor, the number of the cleaved Fc moiety will be reduced, and the redox signal will be higher, due to the inhibition of enzymatic activity. Therefore, the redox wave of the electrochemical reaction of Fc moiety can be correlated with the enzyme reaction, and the detection of DPP-IV activity and screening of its inhibitor is possible with the electrochemical method.

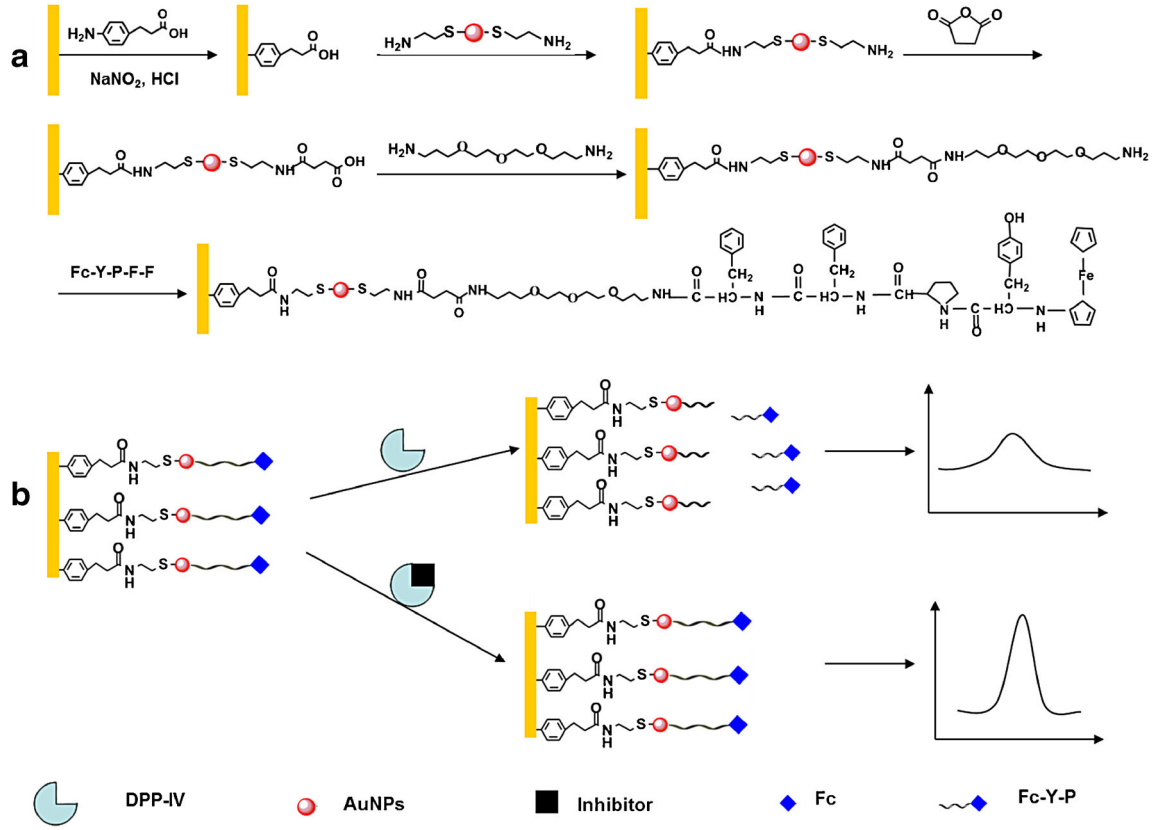

Scheme 1 **a** The fabrication of Fc-peptide modified gold electrode surface. **b** The mechanism of the method for the detection of DPP-IV activity and screening of its inhibitor

Electrochemical characterization of gold electrode surface

As well known, the changes occurring at the electrode surface can be reflected by EIS, which can be used to investigate the chemical transformation and process associated with the electrode surface [21, 22]. In the Nyquist diagram of EIS, the increase of the diameter of the semicircle reflects the increase of the interfacial electron-transfer resistance (R_{et}) [23, 24]. The Nyquist plots of EIS for the electrode at different modified stages are shown in Fig. 1. Nearly no semicircle can be observed for the bare gold electrode (Fig. 1a). After the electrode is modified with APPA, an obviously large semicircle can be detected (Fig. 1b), which is attributed to repulsive interaction between the negatively charged probe, ferrocyanide, and the negatively polarized carboxylic acid groups exposed on the modified electrode surface. When the electrode surface is further modified by CA-AuNPs, an evidently small R_{et} can be tested (Fig. 1c), indicating the decrease of electron transfer resistance. It can be explained by good conductivity of nanoparticles and the attractive interaction between the negatively charged probe and the positively polarized amine group on the surface of nanoparticles. Finally, when Fc-peptide is covalently linked to the electrode surface, the greatest semicircle can be observed (Fig. 1d), because numerous Fc-peptides keep the redox probe from getting access to the electrode surface.

The cyclic voltammograms obtained before and after Fc-peptide/CA-AuNPs/APPA/Au electrode is incubated with the enzyme solution with different concentration are presented in Fig. 2. Prior to the incubation, a pair of well-defined redox

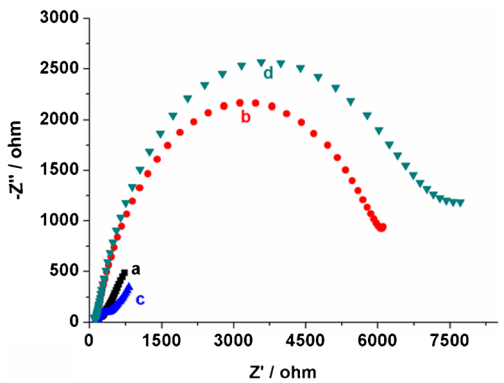

Fig. 1 Nyquist diagrams for the electrochemical impedance measurements of the gold electrode at different modification stage. **a** bare gold electrode, **b** APPA/Au electrode, **c** CA-AuNPs/APPA/Au electrode, **d** Fc-peptide/CA-AuNPs/APPA/Au electrode. Electrochemical species: 5.0 mM $[Fe(CN)_6]^{3-/4-}$. Biasing potential: 0.224 V. Amplitude: 5 mV. Frequency range: 0.1 Hz–10 kHz

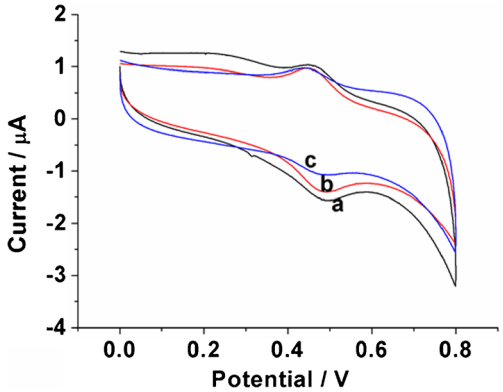

Fig. 2 Cyclic voltammograms obtained after incubation of the Fc-peptide/CA-AuNPs/APPA/Au electrode with 0, 0.5 and 5 mU·mL^{-1} DPP-IV, respectively. Electrolytic solution: 1.0 M $NaClO_4$. Scan rate: 100 mV·s^{-1}

peaks can be observed. The redox peaks with E_{pa}=0.44 V can be ascribed to the oxidation/reduction of the Fc moieties [25, 26]. It also implies that Fc-peptide has been successfully loaded on the electrode surface. After the incubation with DPP-IV solution (0.5 mU·mL^{-1}), the redox peak current significantly decreases, indicating that the number of Fc moiety on the electrode surface decreases, due to the reason that the Fc moiety is cleaved by the enzyme and released from the electrode surface into the bulk solution [27]. Furthermore, the current value decreases along with the increasing enzyme concentration from 0.5 to 5 mU·mL^{-1}, as a result of the cleavage of more Fc-moieties by the enzyme.

Optimization of electrode modification and reaction condition

Both the sensitivity and detection range of the biosensor can be improved with the increasing amount of substrate, Fc-peptide, immobilized on the electrode surface. The amount of the substrate can be detected by the current value. As shown in Fig. S3 (ESM), with the increase of the substrate concentration from 10 to 90 μM, the current value gradually increases. However, the value keeps almost unchanged, when the concentration varies from 90 to 110 μM. Therefore, 90 μM is chosen as the concentration of the Fc-peptide required to be loaded on the electrode surface.

The pH value of the test solution and the reaction temperature may also influence the enzyme activity and the catalytic efficiency, which in the end have a great impact on the sensitivity of the biosensor. With a high enzyme activity, a large amount of Fc-peptide can be cleaved, resulting in a largely decreased current value. As shown in Fig. S4 (ESM), when the pH attains to 7.8, the current value minimizes. Meanwhile, it is found that a minimum value can be observed with 37 °C of the temperature. Thus, 7.8 pH value and 37 °C are separately chosen as the optimized pH and temperature for detection of DPP-IV activity and its inhibitor screening.

Electrochemical detection of DPP-IV activity

The square wave votammograms upon analyzing different concentrations of DPP-IV are shown in Fig. 3a. It can be observed that the peak currents decrease with the increasing concentration of DPP-IV. This is certainly resonable since more products, Fc-Tyr-Pro, can be released from electrode surface to solution in the presence of more enzyme, as a result of the hydrolysis of more substrate Fc-peptides, Fc-Tyr-Pro-Phe-Phe.

The calibration plot obtained for the detection of DPP-IV activity with different concentration is exhibited in Fig. 3b. In the range of 50 nU·mL^{-1}–25 mU·mL^{-1}, the peak current difference decreases with the increasing negative logarithmic value of DPP-IV concentration and follows the regression equation of ΔI=1.778−1.395 × exp(−0.5×(((−log$c$)−6.885)/1.952))^2 (μA, U·mL^{-1}, R^2=0.9995). The detection range is much wider than that reported by Miao and Jiang [28, 29]. Furthermore, the current difference decreases linearly with the

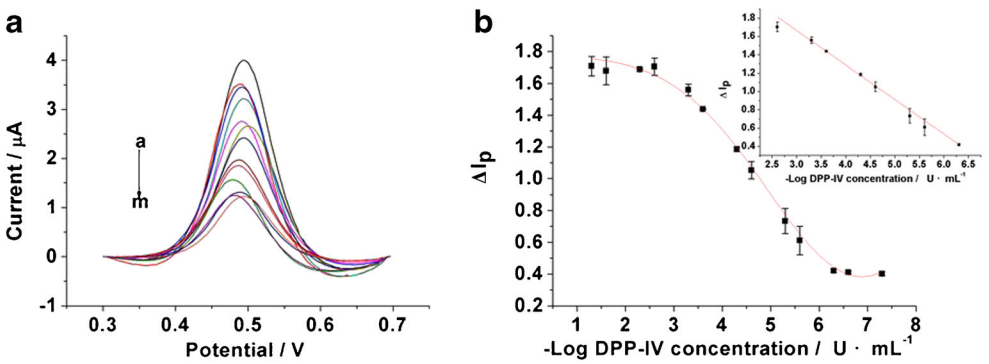

Fig. 3 **a** Square wave voltammograms for the analysis of DPP-IV activity at different concentrations. (*a*) 0, (*b*) 50 nU·mL^{-1}, (*c*) 250 nU·mL^{-1}, (*d*) 0.5 μU·mL^{-1}, (*e*) 2.5 μU·mL^{-1}, (*f*) 5 μU·mL^{-1}, (*g*) 25 μU·mL^{-1}, (*h*) 50 μU·mL^{-1}, (*i*) 250 μU·mL^{-1}, (*g*) 0.5 mU·mL^{-1}, (*k*) 2.5 mU·mL^{-1}, (*l*) 5 mU·mL^{-1} and (*m*) 25 mU·mL^{-1}. **b** Calibration curve corresponding to current difference for negative logarithmic value of variable DPP-IV concentration. *Error bars* represent standard deviations of measurements (n=3). Insert shows the linear relationship between the peak current difference and negative logarithmic value of the DPP-IV concentration

negative logarithmic value of DPP-IV concentration from 0.5 μU·mL^{-1} to 2.5 mU·mL^{-1} and follows the regression equation of ΔI=2.795−(−log$c$) × 0.377 (μA, U·mL^{-1}, R^2= 0.9992). The detection precision has been investigated according to the slope of the regression equation of DPP-IV (from 0.5 μU·mL^{-1} to 2.5 mU·mL^{-1}) obtained from three independent assay processes. The RSD of the three slope is 4.14 %. This result demonstrates that the developed assay method has good precision. The detection limit has also been calculated to be 39 nU·mL^{-1} by the interpolation of the mean plus three times the standard deviation of the zero standards [30, 31].

Inhibition assay

It has been reported that specific DPP-IV inhibition may increase the half-life of total circulating glucagon like peptide-1, decreases plasma glucose, and improves impaired glucose tolerance. As a kind of oral anti-diabetic agents, DPP-IV inhibitor can be able to avoid safety and tolerability issues of conventional agents. In order to test and verify that the developed method can be employed for the screening of DPP-IV inhibitors, two compounds, diprotin A and His-Leu, have been used for this study.

Diprotin A, a competitive inhibitor, is usually used for the reference compound [32]. As shown in Fig. 4a, the current value rapidly raises when the concentration changes from 60 to 100 μM. Then the increased rate becomes slow with the varing concentration from 100 to 130 μM. The maximum inhibitoin of diprotin A is 95.5 % with the IC_{50} value of 93.5 μM. Furthermore, it has also been reported that the peptide His-Leu can competitively inhibit DPP-IV activity [33]. Same as diprotin A, the current first increases fastly with increasing the concentration (Fig. 4b). Then the signal raises at lower rate. The maximum inhibition ratio is 87.2 % with the IC_{50} value of 95.5 μM.

Conclusion

In summary, we have developed an electrochemical method for the detection of DPP-IV activity and screening of its inhibitors. With the immobolization of the designed substrate, Fc-peptide, on gold electrode surface and double signal amplification through both phenyl ring layer and AuNPs, a low detection limit (39 nU·mL^{-1}) and a wide linear detection range (0.5 μU·mL^{-1} to 2.5 mU·mL^{-1}) can be obtained using the established method. Moreover, the method can also be employed for the screening of DPP-IV inhibitors. Compared with the traditional method, this method does not need sophisticated and expensive instrument. Therefore, the method will have a great potential for detection of DPP-IV activity and screening of its inhibitors in the future. This assay is rapid and has a good precision and good selectivity. It may be extended to other peptidases and, possibly, proteases and their inhibitors.

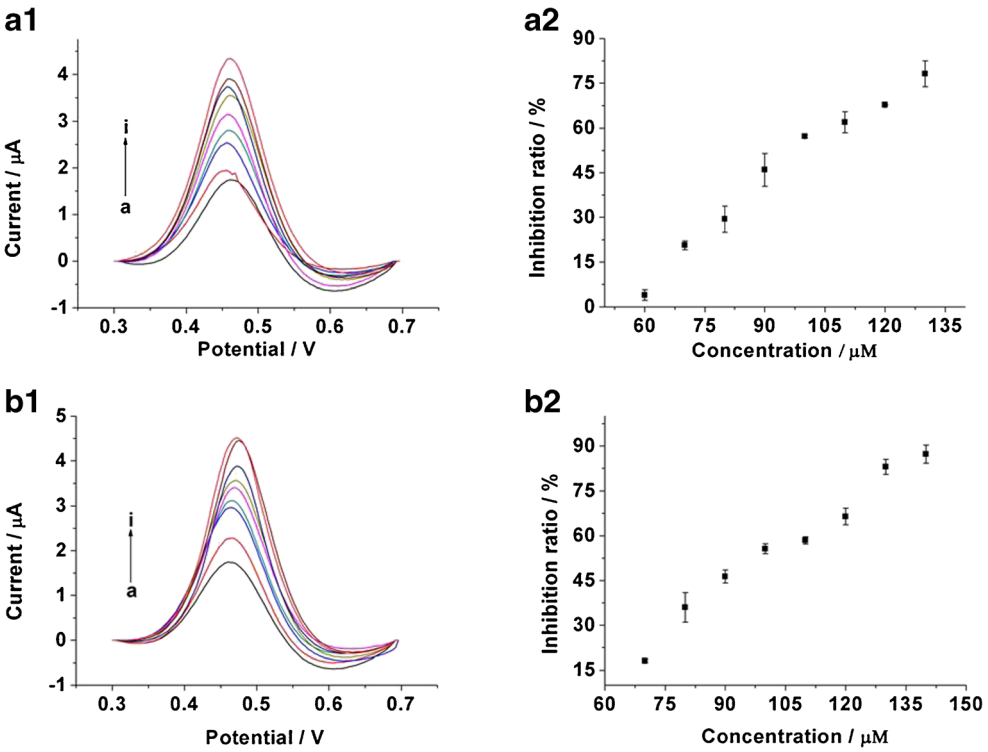

Fig. 4 Square wave voltammograms obtained for Fc-peptide/CA-AuNPs/APPA/Au electrode incubated in DPP-IV solution containing diprotin A (**a1**) and His-Leu peptide (**b1**) with different concentration. The inhibition of diprotin A (**a2**) and His-Leu peptide (**b2**) on DPP-IV activity. Diprotin A concentration: (*a*) 0, (*b*) 60, (*c*) 70, (*d*) 80, (*e*) 90, (*f*) 100, (*g*) 110, (*h*) 120, (*i*) 130 μM. His-Leu peptide concentration: (*a*) 0, (*b*) 70, (*c*) 80, (*d*) 90, (*e*) 100, (*f*) 110, (*g*) 120, (*h*) 130, (*i*) 140 μM. DPP-IV concentration: 2.5 mU·mL^{-1}

Acknowledgments This work is supported by the National Natural Science Foundation of China (Grant Nos. 31101354 and 21235003).

References

1. Juillerat-Jeanneret L (2014) Dipeptidyl peptidase IV and its inhibitors: therapeutics for type 2 diabetes and what else? J Med Chem 57(6):2197–2212. doi:10.1021/jm400658e
2. Shimodaira M, Muroya Y, Kumagai N, Tsuzawa K, Honda K (2013) Effects of short-term intensive glycemic control on insulin, glucagon, and glucagon-like peptide-1 secretion in patients with Type 2 diabetes. J Endocrinol Investig 36(9):734–738. doi:10.3275/8934
3. Holz G (2004) New insights concerning the glucose-dependent insulin secretagogue action of glucagon-like peptide-1 in pancreatic beta-cells. Horm Metab Res 36(11–12):787–794. doi:10.1055/s-2004-826165
4. Durinx C, Lambeir AM, Bosmans E, Falmagne JB, Berghmans R, Haemers A, Scharpe S, De Meester I (2000) Molecular characterization of dipeptidyl peptidase activity in serum–soluble CD26/dipeptidyl peptidase IV is responsible for the release of X-Pro dipeptides. Eur J Biochem 267(17):5608–5613. doi:10.1046/j.1432-1327.2000.01634.x
5. Shane R, Wilk S, Bodnar RJ (1999) Modulation of endomorphin-2-induced analgesia by dipeptidyl peptidase IV. Brain Res 815(2):278–286. doi:10.1016/s0006-8993(98)01121-4
6. Aertgeerts K, Ye S, Shi LH, Prasad SG, Witmer D, Chi E, Sang BC, Wijnands RA, Webb DR, Swanson RV (2004) N-linked glycosylation of dipeptidyl peptidase IV (CD26): effects on enzyme activity, homodimer formation, and adenosine deaminase binding. Protein Sci 13(1):145–154. doi:10.1110/ps.03352504
7. Hama T, Okada M, Kojima K, Kato T, Matsuyama M, Nagatsu T (1982) Purification of dipeptidyl-aminopeptidase IV from human kidney by anti dipeptidyl-aminopeptidase IV affinity chromatography. Mol Cell Biochem 43(1):35–42
8. Kim YB, Kopcho LM, Kirby MS, Hamann LG, Weigelt CA, Metzler WJ, Marcinkeviciene J (2006) Mechanism of Gly-Pro-pNA cleavage catalyzed by dipeptidyl peptidase-IV and its inhibition by saxagliptin (BMS-477118). Arch Biochem Biophys 445(1):9–18. doi:10.1016/j.abb.2005.11.010
9. Swisher LZ, Syed LU, Prior AM, Madiyar FR, Carlson KR, Nguyen TA, Hua DH, Li J (2013) Electrochemical protease biosensor based on enhanced AC voltammetry using carbon nanofiber nanoelectrode arrays. J Phys Chem C 117(8):4268–4277. doi:10.1021/jp312031u
10. Zhang Y, Guo G, Qian Q, Cui D (2012) Chloroplasts-mediated biosynthesis of nanoscale Au-Ag alloy for 2-butanone assay based on electrochemical sensor. Nanoscale Res Lett 7:475–478. doi:10.1186/1556-276x-7-475
11. Syed LU, Liu J, Prior AM, Hua DH, Li J (2011) Enhanced electron transfer rates by AC voltammetry for ferrocenes attached to the end of embedded carbon nanofiber nanoelectrode arrays. Electroanalysis 23(7):1709–1717. doi:10.1002/elan.201100088
12. Mahmoud KA, Hrapovic S, Luong JHT (2008) Picomolar detection of protease using peptide/single walled carbon nanotube/gold nanoparticle-modified electrode. ACS Nano 2(5):1051–1057. doi:10.1021/nn8000774
13. Rónai AZ, Király K, Szebeni A, Szemenyei E, Prohászka Z, Darula Z, Tóth G, Till I, Szalay B, Kató E, Barna I (2009) Immunoreactive endomorphin 2 is generated extracellularly in rat isolated L4,5 dorsal root ganglia by DPP-IV. Regul Pept 157(1–3):1–2. doi:10.1016/j.regpep.2009.06.006
14. Corgier BP, Marquette CA, Blum LJ (2005) Diazonium-protein adducts for graphite electrode microarrays modification: direct and addressed electrochemical immobilization. J Am Chem Soc 127(51):18328–18332. doi:10.1021/ja056946w
15. Olejnik P, Palys B, Kowalczyk A, Nowicka AM (2012) Orientation of laccase on charged surfaces. Mediatorless oxygen reduction on amino- and carboxyl-ended ethylphenyl groups. J Phys Chem 116(49):25911–25918. doi:10.1021/jp3098654
16. Gutiérrez-Sánchez C, Pita M, Vaz-Domínguez C, Shleev S, De Lacey AL (2012) Gold nanoparticles as electronic bridges for laccase-based biocathodes. J Am Chem Soc 134(41):17212–17220. doi:10.1021/ja307308j
17. Zhang Y, Zheng J, Gao G, Kong Y, Zhi X, Wang K, Zhang X, Cui D (2011) Biosynthesis of gold nanoparticles using chloroplasts. Int J Nanomedicine 6:2899–2906. doi:10.2147/ijn.s24785
18. Kim JH, Kim JW, Chung BH (2011) Enzymatic tailoring for precise control of plasmonic resonance absorbance of gold nanoparticle assemblies. J Colloid Interface Sci 360(2):335–340. doi:10.1016/j.jcis.2011.05.008
19. Lyskawa J, Belanger D (2006) Direct modification of a gold electrode with aminophenyl groups by electrochemical reduction of in situ generated aminophenyl monodiazonium cations. Chem Mater 18(20):4755–4763. doi:10.1021/cm060752d
20. Chira A, Covaci OI, Radu GL (2012) A comparative study of gold electrodes modification methods with aromatic compounds based on diazonium and thiol chemistry. Sci Bull B Chem Mater Sci 74(1):183–192
21. Mallesha M, Manjunatha R, Nethravathi C, Suresh GS, Rajamathi M, Melo JS, Venkatesha TV (2011) Functionalized-graphene modified graphite electrode for the selective determination of dopamine in presence of uric acid and ascorbic acid. Bioelectrochemistry 81(2):104–108. doi:10.1016/j.bioelechem.2011.03.004
22. Kang X, Mai Z, Zou X, Cai P, Mo J (2007) A sensitive nonenzymatic glucose sensor in alkaline media with a copper nanocluster/multiwall carbon nano tube-modified glassy carbon electrode. Anal Biochem 363(1):143–150. doi:10.1016/j.ab.2007.01.003
23. Deng C, Chen J, Nie L, Nie Z, Yao S (2009) Sensitive bifunctional aptamer-based electrochemical biosensor for small molecules and protein. Anal Chem 81(24):9972–9978. doi:10.1021/ac901727z
24. Hu C, Yang DP, Wang Z, Yu L, Zhang J, Jia N (2013) Improved EIS performance of an electrochemical cytosensor using three-dimensional architecture Au@BSA as sensing layer. Anal Chem 85(10):5200–5206. doi:10.1021/ac400556q
25. Frasconi M, Mazzei F (2012) Electrochemically controlled assembly and logic gates operations of gold nanoparticle arrays. Langmuir 28(6):3322–3331. doi:10.1021/la203985n
26. Song MJ, Lee SK, Lee JY, Kim JH, Lim DS (2012) Electrochemical sensor based on Au nanoparticles decorated boron-doped diamond electrode using ferrocene-tagged aptamer for proton detection. J Electroanal Chem 677–680:139–144. doi:10.1016/j.jelechem.2012.05.019
27. Liu G, Wang J, Wunschel DS, Lin Y (2006) Electrochemical proteolytic beacon for detection of matrix metalloproteinase activities. J Am Chem Soc 128(38):12382–12383. doi:10.1021/ja0626638
28. Miao L, Lei JY, Jin J, Xu ZH (2009) Establishment and application of screening method for DPP IV inhibitors in vito. Chin Pharmacol Bull 25(3):411–414
29. Jiang HX, Lv JX, Cao Y, Pang JX (2012) Construction of screening model for dipeptidyl peptidase IV in vitro and active inhibitory estimation of related compounds. Chin J Exp Tradit Med Form 18:210–214
30. Cao Y, Wang J, Xu Y, Li G (2010) Combination of enzyme catalysis and electrocatalysis for biosensor fabrication: application to assay the activity of indoleamine 2,3-dioxygensae. Biosens Bioelectron 26(1):87–91. doi:10.1016/j.bios.2010.05.019
31. Hu C, Yang DP, Wang Z, Huang P, Wang X, Chen D, Cui D, Yang M, Jia N (2013) Bio-mimetically synthesized Ag@BSA microspheres as a novel electrochemical biosensing interface for sensitive detection of

tumor cells. Biosens Bioelectron 41:656–662. doi:10.1016/j.bios.2012.09.035

32. Bharti SK, Krishnan S, Kumar A, Rajak KK, Murari K, Bharti BK, Gupta AK (2012) Antihyperglycemic activity with DPP-IV inhibition of alkaloids from seed extract of Castanospermum australe: investigation by experimental validation and molecular docking. Phytomedicine 20(1):24–31. doi:10.1016/j.phymed.2012.09.009
33. Nongonierma AB, FitzGerald RJ (2013) Dipeptidyl peptidase IV inhibitory and antioxidative properties of milk protein-derived dipeptides and hydrolysates. Peptides 39:157–163. doi:10.1016/j.peptides.2012.11.016